Volcanic Influence on European Summer Precipitation through Monsoons: Possible Cause for "Years without Summer"*

MARTIN WEGMANN AND STEFAN BRÖNNIMANN

Oeschger Centre for Climate Change Research and Institute of Geography, University of Bern, Bern, Switzerland

JONAS BHEND

Institute for Atmospheric and Climate Science, ETH Zurich, Zurich, Switzerland, and CSIRO Marine and Atmospheric Research, Aspendale, Victoria, Australia

JÖRG FRANKE

Oeschger Centre for Climate Change Research and Institute of Geography, University of Bern, Bern, Switzerland

DORIS FOLINI AND MARTIN WILD

Institute for Atmospheric and Climate Science, ETH Zurich, Zurich, Switzerland

JÜRG LUTERBACHER

Department of Geography, Climatology, Climate Dynamics and Climate Change, Justus Liebig University of Giessen, Giessen, Germany

(Manuscript received 29 August 2013, in final form 15 January 2014)

ABSTRACT

Strong tropical volcanic eruptions have significant effects on global and regional temperatures. Their effects on precipitation, however, are less well understood. Analyzing hydroclimatic anomalies after 14 strong eruptions during the last 400 years in climate reconstructions and model simulations, a reduction of the Asian and African summer monsoons and an increase of south-central European summer precipitation in the year following the eruption was found. The simulations provide evidence for a dynamical link between these phenomena. The weaker monsoon circulations weaken the northern branch of the Hadley circulation, alter the atmospheric circulation over the Atlantic–European sector, and increase precipitation over Europe. This mechanism is able to explain, for instance, the wet summer in parts of Europe during the "year without a summer" of 1816, which up to now has not been explained. This study underlines the importance of atmospheric teleconnections between the tropics and midlatitudes to better understand the regional climate response to stratospheric volcanic aerosols.

1. Introduction

Explosive tropical volcanic eruptions are a main natural cause of interannual-to-multiannual climate variability and have influenced human societies since the dawn of mankind (Timmreck 2012). Understanding the climate response to volcanic eruptions is important for interpreting past climatic changes (Hegerl et al. 2011), for seasonal climate forecasting after future eruptions, and for the evaluation of climate engineering options (Graf 1992; Trenberth and Dai 2007; Robock et al. 2008). While effects of volcanic eruptions on temperature are well studied (Robock 2000), less is known about the influence on the water cycle. A slowdown of the global water cycle and a decrease of the Asian summer monsoon precipitation was found in previous studies (Gillett et al. 2004; Oman et al. 2006, Trenberth and Dai 2007;

Corresponding author address: Martin Wegmann, Oeschger Centre for Climate Change Research Institute of Geography, University of Bern, Hallerstrasse 12, Bern 3008, Switzerland.
E-mail: martin.wegmann@giub.unibe.ch

Anchukaitis et al. 2010; Joseph and Zeng 2011; Timmreck 2012). Conversely, an increase of summer precipitation is reported for southern Europe based on reconstructions since 1500 (Fischer et al. 2007). The wet summer in parts of Europe following the 1815 Tambora eruption, known as the ''year without a summer'' of 1816, is well documented (Auchmann et al. 2012), but wet summers are also documented for other volcanically perturbed summers such as 1258 (Stothers 2000). Up to now, the mechanisms linking the wet summers to the volcanic eruptions has remained unknown.

In this study, we analyze 14 strong tropical eruptions during the last 400 years. We study the response in statistical reconstructions of boreal summer (June–August) precipitation and temperature in Europe and in summer drought reconstructions for the Asian monsoon region. We then compare the results with a large ensemble of simulations with an atmospheric general circulation model (GCM), which we contrast with simulations from which volcanic aerosols were removed.

2. Data and methods

In the following, we use reconstructions of temperature (Luterbacher et al. 2004) and precipitation (Pauling et al. 2006) for Europe as well as reconstructions of the Palmer drought severity index (PDSI) for the Asian monsoon region. Reconstruction datasets have been used before for studying volcanic influences (Fischer et al. 2007; Anchukaitis et al. 2010).

GCM simulations for the last 400 years (Bhend et al. 2012) were performed using the ECHAM5.4 atmospheric model (Roeckner et al. 2006) at a triangular spectral truncation of T63 and 31 levels in the vertical (model top at 10 hPa). The model was forced with reconstructed and observed monthly mean sea surface temperatures (SSTs). SSTs are based on reconstructed annual temperature (Mann et al. 2009) augmented by El Niño–Southern Oscillation (ENSO)-dependent monthly anomaly fields estimated from the Hadley Centre Sea Ice and Sea Surface Temperature dataset, version 1.1 (HadISST1.1; Rayner et al. 2003). The anomaly fields were derived from regressing monthly SST anomalies onto an annual El Niño index (E. R. Cook, R. D'Arrigo, and K. Anchukaitis 2008, personal communication). Sea ice according to the HadISST climatology is used before 1870 and observed sea ice thereafter (Rayner et al. 2003).

Volcanic forcing is computed online as in Jungclaus et al. (2010) based on reconstructions by Crowley et al. (2008), consisting of aerosol optical depth (AOD) at $0.55 \,\mu m$ and effective particle radii in four latitude bands. AOD is distributed across three layers of the stratosphere between 70 and 30 hPa with a maximum at 50 hPa. Using

AOD, effective radii, and normalized optical parameters, radiative properties of volcanic aerosols are computed for the six solar bands (0.185–$4\,\mu m$) and extinction is computed for the 16 longwave bands (3.3–$100\,\mu m$) in the ECHAM5 radiation scheme (Roeckner et al. 2003). The computed normalized parameters are dependent on lognormal aerosol size distribution with a constant standard deviation of 1.8 logarithmic units and an effective radius between 0.02 and $1\,\mu m$.

Furthermore, the model was forced by observed greenhouse gases (Yoshimori et al. 2010), tropospheric aerosols (Koch et al. 1999), total solar irradiance (Lean 2000), and land surface conditions (Pongratz et al. 2008). Unfortunately, there was a misspecification of long-term changes in land surface properties. However, this does not affect the results presented here, as summers after volcanic eruptions are compared either to the same years in other simulations or to an adjacent climatology. Moreover, the general circulation is not strongly affected. Because of problems with excessive model wind speed over Antarctica, at times causing wavelike patterns, global fields (and analyzed on a $4° \times 4°$ grid) were cut at 60°S.

Using the described setup, a 30-member initial-condition ensemble of model simulations was forced with all relevant forcings (termed ALL) from 1599 to 2005. In addition, 30-member ensemble simulations were also performed for each eruption year (and the following 5 years) with the same forcings as in ALL except that volcanic aerosols were set to background conditions (named NOVOLC).

For consistency, a list of volcanic eruptions was derived from the literature (Shindell et al. 2004; Fischer et al. 2007; Anchukaitis et al. 2010) and modulated, so that it contains 14 explosive eruptions that very likely affected the stratosphere and thus are relevant for extended global climate impacts near the ground (Table 1). Note that the definition of a volcanic-influenced season may vary among the studies mentioned above. A reference climatology was constructed for each eruption (both in the ALL and in the reconstructions) consisting of 10 seasons before and 10 seasons after the eruption (except for the eruption in 1600, where the following 20 seasons were used). Within the climatology, summers following volcanic eruptions were omitted.

The influence of an eruption can, on the one hand, be expressed as the difference between the following summer and all summers from a reference period around the eruption (named ALL-REF in model analyses). This allows for comparison between model results and reconstructions. On the other hand, in the GCM only, the volcanic influence can also be expressed as the difference between ALL and NOVOLC. In the latter case, any atmospheric effects resulting from SST variations (including

TABLE 1. Names, dates, and characteristics of the volcanic eruptions investigated. Global AOD is from Crowley et al. (2008) and refers to the corresponding summer. ENSO is based on Brönnimann et al. (2007) and refers to the boreal winter preceding the summer analyzed. In the ENSO column, the symbols ++, +, and 0 denote extreme El Niño events, strong El Niño events, and weak ENSO or neutral conditions, respectively (none of the summers coincided with extreme or strong La Niña events). Southern European precipitation (precip.) anomalies are averages over the land area (36°–46°N, 10°W–40°E). Shown are differences calculated for each eruption relative to a reference period around each eruption (see section 2) in the model (ALL-REF) and in the reconstructions (rec.).

Eruption date in model	Name	First summer	Global AOD (JJA)	ENSO	European precip. model (JJA) (mm day^{-1})	European precip. rec. (JJA) (mm day^{-1})
January 1600	Huaynaputina	1600	0.181	0	0.147	−0.266
January 1641	Parker	1641	0.185	0	0.143	0.327
May 1673	Gamkonora	1674	0.122	+	−0.004	0.619
April 1694	Serua	1695	0.137	0	0.064	0.674
February 1809	unknown	1809	0.247	0	0.076	0.160
April 1815	Tambora	1816	0.358	+	0.062	0.715
October 1831	Babuyan Claro	1832	0.115	0	0.095	−0.317
January 1835	Cosiguina	1836	0.151	0	0.010	0.396
December 1861	Dubbi	1862	0.067	0	0.026	−0.332
August 1883	Krakatau	1884	0.180	0	0.091	0.866
October 1902	Santa Maria	1903	0.083	+	−0.005	0.647
March 1963	Agung	1963	0.048	0	−0.032	−0.306
April 1982	El Chichón	1983	0.074	++	0.011	0.450
June 1991	Pinatubo	1992	0.134	+	−0.028	0.726

possible volcanic imprints on SSTs; see Zanchettin et al. 2013) are not captured as the same SSTs are used in ALL and NOVOLC. In the following, we focus on averaged differences over all 14 eruptions. Significance was calculated using a one-sample *t* test of the differences for each eruption (based on ensemble means in case of model data). Field significance was tested according to Ventura et al. (2004).

3. Results

Tree ring–based climate reconstructions show an increase in drought severity (negative PDSI) in large parts of East Asia in summers following tropical eruptions (Fig. 1a; also found by Anchukaitis et al. 2010), but with anomaly patterns reacting sensibly to the timing of the eruption and definition of the summer after the eruption. Drought also increases over central India and Indonesia, but decreases in the regions bordering the Sea of Japan. In southern Europe, an increase in summer precipitation is shown, with negative anomalies northeast of the Mediterranean region (similar to Fischer et al. 2007). However, the overall tendency is positive for southern European precipitation anomalies. The model simulations (ALL-REF) show significantly reduced summer precipitation in Asia, consistent with increased drought (Fig. 1c), and significantly increased precipitation in south-central Europe. The model response in the latter case is weaker than in the reconstructions (Fig. 1d). The Southern European response is seen after 10 out of 14 eruptions (Table 1).

Winter temperature and precipitation anomalies in Europe are similarly well reproduced by the model (Fig. 2; see Fig. S1 in the supplemental material for global fields). The warming over northeastern Europe (see also Robock and Mao 1992; Fischer et al. 2007) is highly significant in the model and contrasts recent coupled climate model simulations (Driscoll et al. 2012). The north–south gradient in precipitation is reproduced qualitatively, though it is weaker than in reconstructions. This comparison increases the confidence that the ECHAM5.4 atmospheric model simulations are capable of reproducing the important dynamic features after volcanic eruptions.

Globally, boreal summer seasons following volcanic eruptions are characterized in the model by a decrease of precipitation over continental equatorial regions and in monsoon areas, similar to Joseph and Zeng (2011), and an increase over subtropical oceans (Fig. 3). Both analyses (ALL-REF and ALL-NOVOLC) yield essentially the same result, suggesting that the climate response during the first summer following an eruption can largely be explained by volcanic impacts only. In the following, we focus on ALL-NOVOLC analyses; results for ALL-REF are presented in the supplemental material.

Precipitation can be affected through changes in evaporation and atmospheric circulation. In the simulations, evaporation is reduced after eruptions because of reduced surface solar radiation mainly over the continents (Fig. 4b). In contrast, evaporation significantly increases over the midlatitude North Atlantic and North Pacific storm track regions. Atmospheric circulation,
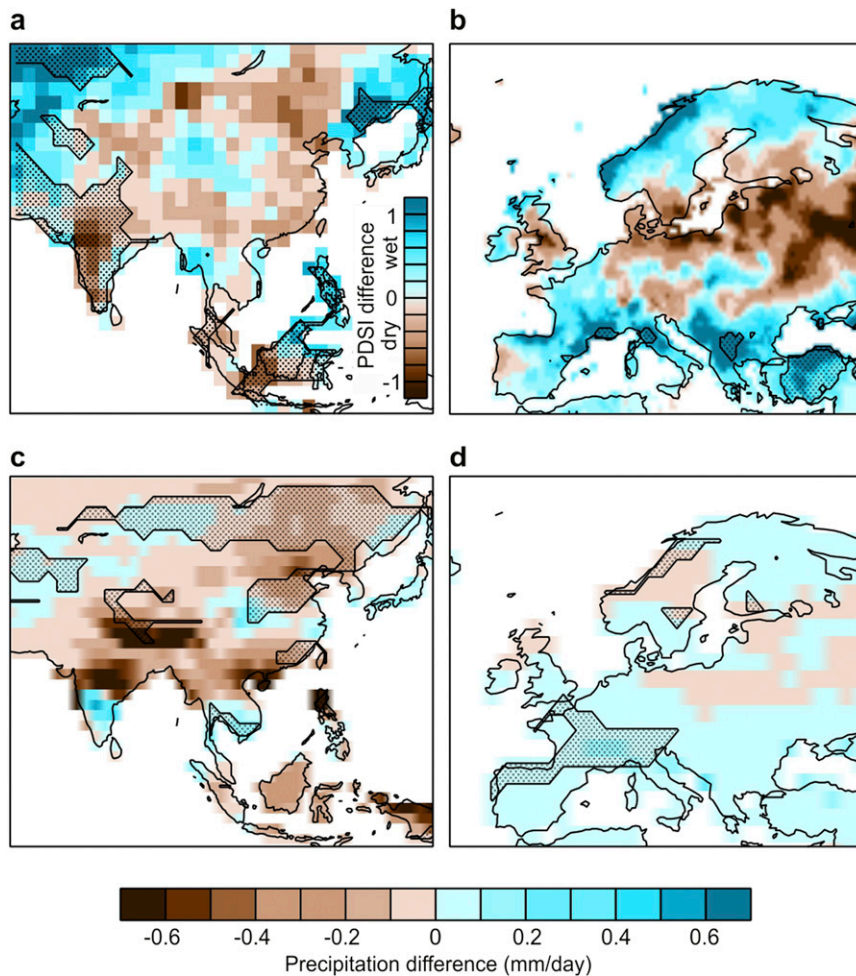
FIG. 1. Boreal summer hydroclimatic anomalies averaged across 14 tropical volcanic erup-
tions. (a),(b) Difference based on statistical climate reconstructions between summers fol-
lowing volcanic eruptions and reference climatologies [PDSI is shown in (a)] and (c),(d)
ensemble mean difference in ECHAM5.4 climate model simulations (composite of 420 sim-
ulated eruptions). Differences are with respect to reference periods around each eruption
(ALL-REF). Stippled areas represent significant differences (t test, 95% confidence level). All
difference fields except (b) are field significant.

analyzed with 500-hPa geopotential heights and 850-hPa
wind vectors (Figs. 4c,d), shows a weakening of the West
African and East Asian monsoon circulations. West-
erlies increase over the subtropical North Atlantic and
subtropical Pacific and decrease over the midlatitudes.

The weakening of the monsoon circulations has been
interpreted in previous studies as a consequence of re-
duced land–sea thermal contrasts (Joseph and Zeng
2011). The reduced solar radiation causes an overall
reduction of temperature and evaporation over the
continents. The cooling of the landmasses is stronger
than that of the oceans because of the different heat
capacity and thereby is weakening atmospheric circu-
lation and hence moisture flux. The reduced latent heat
release in the free troposphere further weakens the

circulation. This mechanism is consistent with our model
simulations (Figs. 4a, S2), although SSTs do not react to
forcing in our model. Embedded in the large-scale
cooling, a weak warming below 850 hPa appears over
central Africa and southern Asia in summers following
eruptions, which was noted in previous studies (Joseph
and Zeng 2011). This surface warming is caused by the
locally increased shortwave radiation, resulting from
the reduction in cloud cover, and a decrease in surface
evaporation. However, cooling dominates in the free
troposphere over the tropics.

Until now, there has been no satisfying explanation
for the posteruption summer precipitation increase over
south-central Europe, which was documented for in-
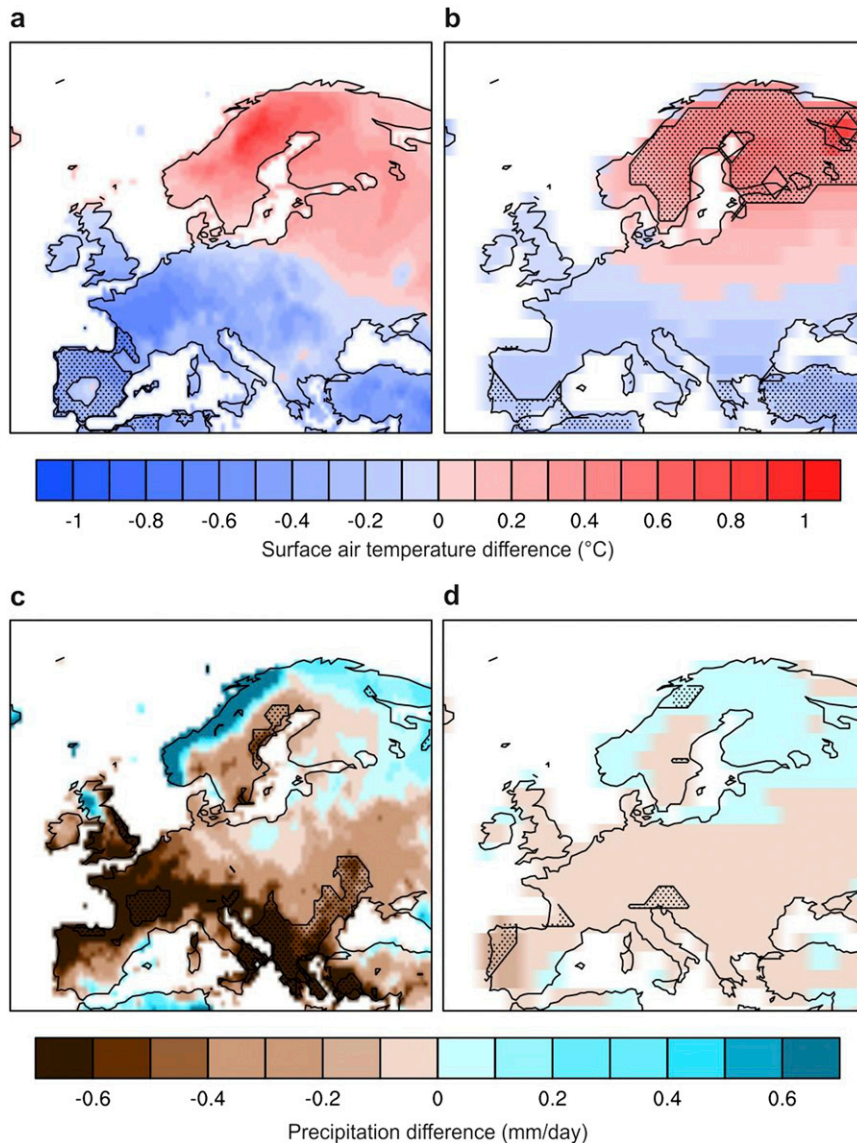dividual cases such as the summer of 1816 following the

FIG. 2. Boreal winter (December–February) temperature and precipitation anomalies averaged across 14 tropical volcanic eruptions. (a),(c) Difference from statistical climate reconstructions and (b),(d) ensemble mean difference in ECHAM5.4 climate model simulations (composite of 420 simulated eruptions). Differences are calculated for each eruption relative to a reference period around each eruption, and then averaged across all 14 eruptions (ALL–REF). Stippled areas represent significant differences (*t* test, 95% confidence level). Only (b) is field significant (95% confidence level).

Tambora eruption (Auchmann et al. 2012) or the 1258 eruption (Stothers 2000; see supplemental material for reconstruction and model response in summer 1816). In the model simulations, the meridional pressure gradient in the eastern North Atlantic is weakened in summer, resembling a negative phase of the North Atlantic Oscillation (Fig. 4c). This causes a southward shift of the storm track (Fig. 4d) and extended moisture advection toward southern Europe. Anomalous uplift over the

eastern Mediterranean Sea, increasing convection, is indicated by the response in vertical velocity (Fig. 4c).

Recent studies have suggested a link between circulation changes over the North Atlantic and changes in the African monsoon system (Gaetani et al. 2011). The mechanism proposes that a weakening of the West African monsoon, with decreased convection in the Sudan–Sahel region, weakens the Hadley cell and leads to weaker subsidence over the eastern Mediterranean and
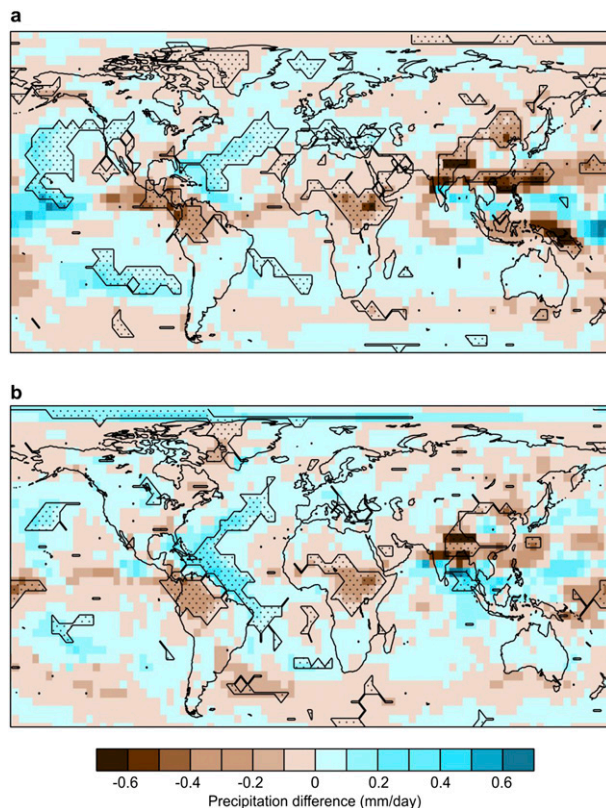
FIG. 3. Boreal summer (June–August) precipitation anomalies averaged across 14 tropical volcanic eruptions in ECHAM5.4 climate model simulations (composite of 420 simulated eruptions) for (a) ALL-REF (ensemble mean differences are calculated for each eruption relative to a reference period around each eruption, then averaged across all eruptions) and (b) ALL-NOVOLC (differences between an ensemble simulation with an ensemble simulation without stratospheric volcanic aerosols, averaged across all ensemble members and eruptions). Stippled areas represent significant differences (t test, 95% confidence level). Both (a) and (b) are field significant (95% confidence level).

a change of the atmospheric flow over the North Atlantic (Gaetani et al. 2011). To explore whether this mechanism is responsible also for the volcanic signature in European summer precipitation, we compared an area average of southern European land precipitation (36°–46°N, 10°W–40°E) with an area average of zonal and meridional wind profiles over Africa (14°–36°N, 25°W–55°E). We analyzed the average difference as well as the interevent correlations in the ensemble mean (Fig. 5). The average difference for ALL-NOVOLC shows negative zonal and meridional wind anomalies over Africa up to the 400-hPa level and positive anomalies in the upper troposphere (the same is found for ALL-REF, not shown). Almost all individual eruptions (gray lines) reveal a similar pattern, which corresponds to a weakened West African monsoon flow near the surface, a strengthened African easterly jet in the lower

troposphere, and a weakened tropical easterly jet in the upper troposphere. Moreover, the interevent correlation shows a very similar vertical profile as the mean anomaly (Figs. 5c,f), with several pressure levels exhibiting significant correlations. This confirms that those eruptions that have a strong effect on the African monsoons also have a strong effect on southern European summer precipitation.

4. Discussion

Our results are consistent with a physical link between the African and Asian monsoons and summer precipitation over southern Europe (Gaetani et al. 2011; Tyrlis et al. 2013) triggered by volcanic eruptions. This relationship propagates through a weakened northern Hadley cell (imprinted in the difference in 500-hPa vertical velocity; see Figs. 4, S2) and associated change in the pressure distribution over the North Atlantic–European sector. Thus, a physically consistent mechanism is established of how tropical volcanic eruptions affect European summer precipitation. This European posteruption precipitation signal is detected in reconstruction and the model dataset (see supplemental material for statistical assessment of intraensemble variability).

The suggested mechanism operates via the reduction of incoming radiation at the Earth's surface by stratospheric volcanic aerosols. In contrast, the winter warming over northeastern Europe (and the precipitation decrease over southwestern Europe; Fig. 2) is likely related to stratospheric dynamical effects of the aerosols and subsequent downward propagation, leading to increased zonal flow over the North Atlantic–European region (Robock 2000). Additional mechanisms may possibly contribute to the summer response. For instance, the change in temperature and wind shear in the tropical lowermost stratosphere after volcanic eruptions might affect the upper limit of deep convection in the western tropical Pacific, from where influences on the monsoons as well as on the extratropical circulation might develop (similar to that suggested with respect to the quasi-biennial oscillation; Giorgetta and Bengtsson 1999). This mechanism remains to be analyzed in subsequent studies.

The influence of further possible shortcomings of the simulations (variance changes in SSTs used as boundary conditions, representation of precipitation variability, and overestimation of stratospheric temperature signal) was analyzed, but none of these possible shortcomings is expected to affect our results (details given in the supplemental material).

Additional questions concern the influence of volcanic eruptions on the coupled climate system. The current experimental setup with fixed lower boundary conditions (SSTs) allows us to specifically address the
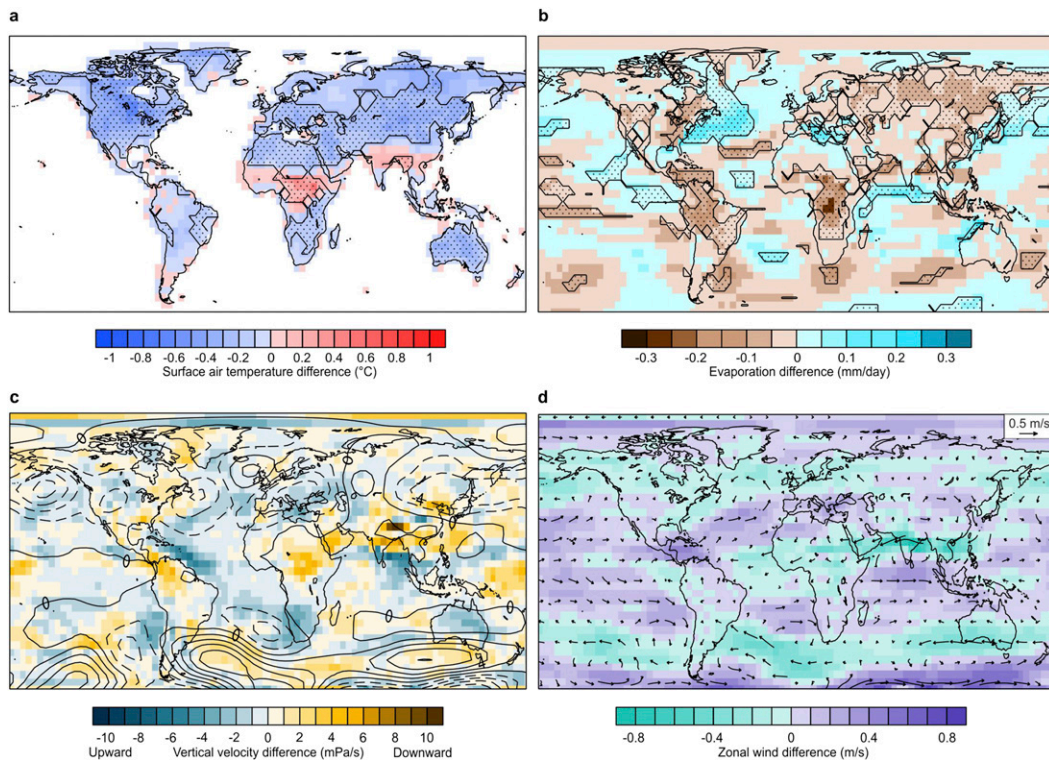
FIG. 4. Boreal summer response to volcanic eruptions in ECHAM5.4 climate model simulations averaged across 14 eruptions for (a) surface air temperature, (b) evaporation (positive values denote an upward flux), (c) vertical velocity (colors) and geopotential height (contour interval is 2 gpm, dashed contours are negative) at 500 hPa, and (d) wind vectors and zonal wind at 850 hPa. Plotted are differences between ALL and NOVOLC simulations. Stippled areas in (a) and (b) represent significant differences (*t* test, 95% confidence level). All difference fields are field significant.

atmospheric response to volcanic eruptions independent of (volcanically forced) SST variability. The response of the coupled climate system such as delayed winter–spring signatures (Zanchettin et al. 2013; Zhang et al. 2013) or the increased occurrence of El Niño events (Fig. S3 in the supplemental material) after volcanic eruptions, on the other hand, cannot be analyzed in the current setup, but require the use of coupled ocean–atmosphere models. Conversely, the increased occurrence of El Niño events after volcanic eruptions does not affect the ALL-NOVOLC analysis and therefore cannot explain the results. Whether a more realistic representation of the stratosphere would change the result remains open. Existing studies (Driscoll et al. 2012; Charlton-Perez et al. 2013) imply that an increase in stratospheric resolution and model top does not necessarily increase the ability to reproduce volcanic induced climate anomalies. Nevertheless, future multimodel studies are needed to exclude any model dependency.

5. Conclusions

In this study we have addressed regional precipitation effects of tropical volcanic eruptions in the Asian and African monsoon regions and in Europe in boreal summer. We found a weakening of the monsoons, but an increase in European summer precipitation in reconstructions and a climate model. The model provides evidence that the wet European summers are linked to the weakened African monsoon via changes in the Hadley cell.

Understanding the variability of monsoon rains as well as their predictability is important as large parts of the world's food security depend on this climatic feature. Hence, better understanding the relation between monsoon and stratospheric aerosols is not only relevant for preparing for future volcanic eruptions, but potentially also for the evaluation of climate engineering options. Our results indicate that the influence of stratospheric volcanic aerosols on the monsoon system, through triggering continental-scale circulation feedbacks, have distinct effects on regional precipitation. The suggested mechanism is also able to explain the wet conditions in Europe during the "year without a summer" of 1816 and arguably similar past volcanic episodes as a consequence of altered monsoons.
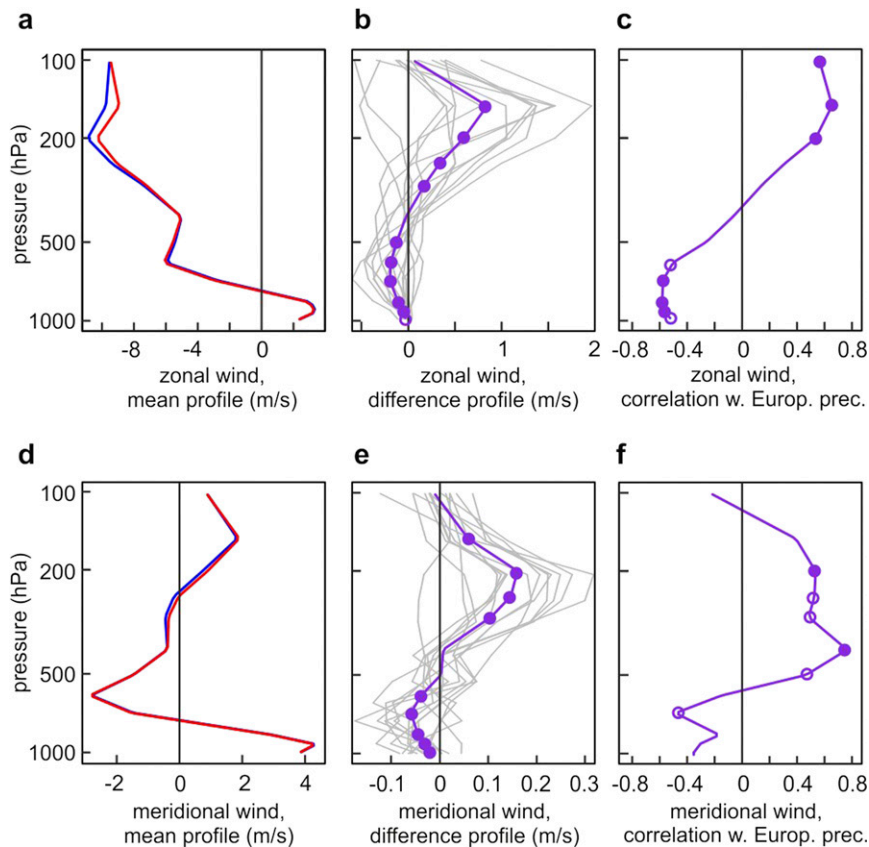
FIG. 5. West African monsoon and European summer precipitation following volcanic eruptions in ECHAM5.4 simulations. (top) Zonal and (bottom) meridional wind profiles averaged over the West African monsoon region (14°–36°N, 25°W–55°E). (a),(d) Ensemble mean over all 14 eruptions for NOVOLC (blue) and ALL (red). (b),(e) Difference between ALL and NOVOLC (purple; gray lines show results for each individual eruption). (c),(f) Intereruption Pearson correlation of ensemble mean precipitation anomalies (ALL minus NOVOLC) over southern European land areas (36°–46°N, 10°W–40°E) with corresponding wind anomalies in the West African monsoon region. Open and closed circles denote significance at the 90% and 95% confidence levels, respectively.

REFERENCES

Anchukaitis, K. J., B. M. Buckley, E. R. Cook, B. I. Cook, R. D. D'Arrigo, and C. M. Ammann, 2010: Influence of volcanic eruptions on the climate of the Asian monsoon region. *Geophys. Res. Lett.,* **37,** L22703, doi:10.1029/2010GL044843.

Auchmann, R., S. Brönnimann, L. Breda, M. Bühler, R. Spadin, and A. Stickler, 2012: Extreme climate, not extreme weather: The summer 1816 in Geneva, Switzerland. *Climate Past,* **8,** 325–335, doi:10.5194/cp-8-325-2012.

Bhend, J., J. Franke, D. Folini, M. Wild, and S. Brönnimann, 2012: An ensemble-based approach to climate reconstructions. *Climate Past,* **8,** 963–976, doi:10.5194/cp-8-963-2012.

Brönnimann, S., E. Xoplaki, C. Casty, A. Pauling, and J. Luterbacher, 2007: ENSO influence on Europe during the last centuries. *Climate Dyn.,* **28,** 181–197, doi:10.1007/s00382-006-0175-z.

Charlton-Perez, A. J., and Coauthors, 2013: On the lack of stratospheric dynamical variability in low-top versions of the CMIP5 models. *J. Geophys. Res. Atmos.,* **118,** 2494–2505, doi:10.1002/jgrd.50125.

Crowley, T., G. Zielinski, B. Vinther, R. Udisti, K. Kreutz, J. Cole-Dai, and E. Castellano, 2008: Volcanism and the Little Ice Age. PAGES News, Vol. 16, No. 2, International Geosphere-Biosphere Programme, Bern, Switzerland, 22–23. [Available

online at http://pages-142.unibe.ch/products/newsletters/2008-2/Special%20Section/Science%20Highlights/Crowley_2008-2(22-23).pdf.]

Driscoll, S., A. Bozzo, L. J. Gray, A. Robock, and G. Stenchikov, 2012: Coupled Model Intercomparison Project 5 (CMIP5) simulations of climate following volcanic eruptions. *J. Geophys. Res.,* **117,** D17105, doi:10.1029/2012JD017607.

Fischer, E. M., J. Luterbacher, E. Zorita, S. F. B. Tett, C. Casty, and H. Wanner, 2007: European climate response to tropical volcanic eruptions over the last haft millennium. *Geophys. Res. Lett.,* **34,** L05707, doi:10.1029/2006GL027992.

Gaetani, M., B. Pohl, H. Douville, and B. Fontaine, 2011: West African monsoon influence on the summer Euro-Atlantic circulation. *Geophys. Res. Lett.,* **38,** L09705, doi:10.1029/2011GL047150.

Gillett, N. P., A. J. Weaver, F. W. Zwiers, and M. F. Wehner, 2004: Detection of volcanic influence on global precipitation. *Geophys. Res. Lett.,* **31,** L12217, doi:10.1029/2004GL020044.

Giorgetta, M. A., and K. A. Bengtsson, 1999: An investigation of QBO signals in the east Asian and Indian monsoon in GCM experiments. *Climate Dyn.,* **15,** 435–450, doi:10.1007/s003820050292.

Graf, H.-F., 1992: Arctic radiation deficit and climate variability. *Climate Dyn.,* **7,** 19–28, doi:10.1007/BF00204818.

Hegerl, G., J. Luterbacher, F. González-Rouco, S. F. B. Tett, T. Crowley, and E. Xoplaki, 2011: Influence of human and natural forcing on European seasonal temperatures. *Nat. Geosci.,* **4,** 99–103, doi:10.1038/ngeo1057.

Joseph, R., and N. Zeng, 2011: Seasonally modulated tropical drought induced by volcanic aerosol. *J. Climate,* **24,** 2045–2060, doi:10.1175/2009JCLI3170.1.

Jungclaus, J. H., and Coauthors, 2010: Climate and carbon-cycle variability over the last millennium. *Climate Past,* **6,** 1009–1044, doi:10.5194/cpd-6-1009-2010.

Koch, D., D. Jacob, I. Tegen, D. Rind, and M. Chin, 1999: Tropospheric sulfur simulation and sulfate direct radiative forcing in the Goddard Institute for Space Studies general circulation model. *J. Geophys. Res.,* **104,** 23 799–23 822, doi:10.1029/1999JD900248.

Lean, J., 2000: Evolution of the suns spectral irradiance since the Maunder minimum. *Geophys. Res. Lett.,* **27,** 2425–2428, doi:10.1029/2000GL000043.

Luterbacher, J., D. Dietrich, E. Xoplaki, M. Grosjean, and H. Wanner, 2004: European seasonal and annual temperature variability, trends and extremes since 1500. *Science,* **303,** 1499–1503, doi:10.1126/science.1093877.

Mann, M., J. Woodruff, J. Donnelly, and Z. Zhang, 2009: Atlantic hurricanes and climate over the past 1500 years. *Nature,* **460,** 880–883, doi:10.1038/nature08219.

Oman, L., A. Robock, G. L. Stenchikov, and T. Thordarson, 2006: High-latitude eruptions cast shadow over the African monsoon and the flow of the Nile. *Geophys. Res. Lett.,* **33,** L18711, doi:10.1029/2006GL027665.

Pauling, A., J. Luterbacher, C. Casty, and H. Wanner, 2006: Five hundred years of gridded high-resolution precipitation reconstructions over Europe and the connection to large-scale circulation. *Climate Dyn.,* **26,** 387–405, doi:10.1007/s00382-005-0090-8.

Pongratz, J., C. Reick, T. Raddatz, and M. A. Claussen, 2008: A reconstruction of global agricultural areas and land cover for

the last millennium. *Global Biogeochem. Cycles,* **22,** GB3018, doi:10.1029/2007GB003153.

Rayner, N., D. E. Parker, E. B. Horton, C. K. Folland, L. V. Alexander, D. P. Rowell, E. C. Kent, and A. Kaplan, 2003: Global analysis of sea surface temperature, sea ice, and night maritime air temperature since the late nineteenth century. *J. Geophys. Res.,* **108,** 4407, doi:10.1029/2002JD002670.

Robock, A., 2000: Volcanic eruptions and climate. *Rev. Geophys.,* **38,** 191–219, doi:10.1029/1998RG000054.

——, and J. Mao, 1992: Winter warming from large volcanic eruptions. *Geophys. Res. Lett.,* **19,** 2405–2408, doi:10.1029/92GL02627.

——, L. Oman, and G. L. Stenchikov, 2008: Regional climate responses to geoengineering with tropical and Arctic SO_2 injections. *J. Geophys. Res.,* **113,** D16101, doi:10.1029/2008JD010050.

Roeckner, E., and Coauthors, 2003: The atmospheric general circulation model ECHAM5. Part I: Model description. Max Planck Institute for Meteorology Rep. 349, 127 pp. [Available online at https://www.mpimet.mpg.de/fileadmin/publikationen/Reports/max_scirep_349.pdf.]

——, and Coauthors, 2006: Sensitivity of simulated climate to horizontal and vertical resolution in the ECHAM5 atmosphere model. *J. Climate,* **19,** 3771–3791, doi:10.1175/JCLI3824.1.

Shindell, D., G. Schmidt, M. Mann, and G. Faluvegi, 2004: Dynamic winter climate response to large tropical volcanic eruptions since 1600. *J. Geophys. Res.,* **109,** D05104, doi:10.1029/2003JD004151.

Stothers, R. B., 2000: Climatic and demographic consequences of the massive voclanic eruption of 1258. *Climatic Change,* **45,** 361–374, doi:10.1023/A:1005523330643.

Timmreck, C., 2012: Modeling the climatic effects of large explosive volcanic eruptions. *Wiley Interdiscip. Rev.: Climate Change,* **3,** 545–564, doi:10.1002/wcc.192.

Trenberth, K. E., and A. Dai, 2007: Effects of Mount Pinatubo volcanic eruption on the hydrological cycle as an analog of geoengineering. *Geophys. Res. Lett.,* **34,** L15702, doi:10.1029/2007GL030524.

Tyrlis, E., J. Lelieveld, and B. Steil, 2013: The summer circulation over the eastern Mediterranean and the Middle East: Influence of the South Asian monsoon. *Climate Dyn.,* **40,** 1103–1123, doi:10.1007/s00382-012-1528-4.

Ventura, V., C. J. Paciorek, and J. S. Risbey, 2004: Controlling the proportion of falsely rejected hypotheses when conducting multiple tests with climatological data. *J. Climate,* **17,** 4343–4356, doi:10.1175/3199.1.

Yoshimori, M., C. Raible, T. Stocker, and M. Renold, 2010: Simulated decadal oscillations of the Atlantic meridional overturning circulation in a cold climate state. *Climate Dyn.,* **34,** 101–121, doi:10.1007/s00382-009-0540-9.

Zanchettin, D., O. Bothe, H. F. Graf, S. J. Lorenz, J. Luterbacher, C. Timmreck, and J. H. Jungclaus, 2013: Background conditions influence the decadal climate response to strong volcanic eruptions. *J. Geophys. Res. Atmos.,* **118,** 4090–4106, doi:10.1002/jgrd.50229.

Zhang, D., R. Blender, and K. Fraedrich, 2013: Volcanoes and ENSO in millennium simulations: Global impacts and regional reconstructions in East Asia. *Theor. Appl. Climatol.,* **111,** 437–454, doi:10.1007/s00704-012-0670-6.